metals

MDPI

Article

Hydrogen Diffusion Mechanism around a Crack Tip in Type 304L Austenite Stainless Steel Considering the Influence of the Volume Expansion of Strain-Induced Martensite Transformation

Zhiliang Xiong [1,2], Wenjian Zheng [1,3,*], Yanzhang Liu [1,2], Yanjun Kuang [1,2] and Jianguo Yang [3]

1 State Key Laboratory of Nuclear Power Safety Monitoring Technology and Equipment, China Nuclear Power Engineering Co., Ltd., Shenzhen 518172, China
2 China Nuclear Power Design Co., Ltd (Shenzhen), Shenzhen 518172, China
3 Institute of Process Equipment and Control Engineering, Zhejiang University of Technology, Hangzhou 310014, China
* Correspondence: zwj0322@zjut.edu.cn; Tel.: +86-571-8887-1059; Fax: +86-571-8832-0842

Received: 28 July 2019; Accepted: 2 September 2019; Published: 3 September 2019

Abstract: Strain-induced martensite transformation (SIMT) commonly exists around a crack tip of metastable austenite stainless steels. The influence of the volume expansion of the SIMT on the hydrogen diffusion was investigated by hydrogen diffusion modeling around a crack tip in type 304L austenite stainless steel. The volume expansion changed the tensile stress state into pressure stress state at the crack tip, resulting in a large stress gradient along the crack propagation direction. Compared to the analysis without considering the volume expansion effect, this volume expansion further accelerated the hydrogen transport from the inner surface to a critical region ahead of the crack tip, and further increased the maximum value of the hydrogen concentration at the critical position where the strain-induced martensite fraction approximates to 0.1, indicating that the volume expansion of the SIMT further increased the hydrogen embrittlement susceptibility.

Keywords: hydrogen diffusion; strain-induced martensite transformation; crack tip; austenite stainless steel

1. Introduction

Due to the high resistance to hydrogen embrittlement (HE) and low hydrogen diffusivity, austenite stainless steels (ASSs) have been widely used in hydrogen-containing environments. The metastable ASSs, such as type 301, 304(L) and 316, usually undergo suitable cold work process to reach higher strength and better resistance to HE and stress corrosion cracking [1,2]. However, excessive cold work reverses this effect due to the over-occurrence of strain-induced martensite (α'-martensite and ε-martensite) transformation (SIMT) [3], since the strain-induced martensite is much more sensitive than austenite to hydrogen [4,5]. Therefore, HE generally occurs as the results of hydrogen-induced crack initiation and propagation during the process of SIMT [6,7].

Investigating the hydrogen diffusion around a crack tip is critical to predict and prevent the hydrogen assisted crack. Thus, a lot of the literature focused on analyzing the hydrogen diffusion around a crack tip. Sofronis and McMeeking [8] established the basis of hydrogen diffusion near a blunting crack tip, where the maximum lattice hydrogen concentration is at the distance of the peak site of the hydrostatic stress from the crack tip. However, in comparison with the population of the trapping site's hydrogen, the lattice diffusion is very small. Yokobori et al. [9] constructed a physical and numerical analysis to describe the hydrogen concentration evolution around a crack tip

considering the stress assisted diffusion. Liang et al. [10] conducted numerical simulation of hydrogen diffusion considering the stress, plastic strain and hydrogen-induced reduction of interfacial cohesion and material softening. Takakuwa et al. [11] used finite element (FE) analysis to show the influence of the residual stress on the hydrogen concentration around a crack tip in plastically deformable material after a fatigue process. Paneda et al. [12] examined the hydrogen diffusion towards the fracture process zone accounting for local hardening due to geometrically necessary dislocation by means of strain gradient plasticity. Unlike plasticity-base prediction, the increased dislocation density associated with gradients of plastic strain caused very high levels of crack tip lattice hydrogen concentration.

For the crack tip in metastable ASSs, the material and mechanical behaviors are entirely different. In the absence of hydrogen, the martensite transformation can result in a pronounced crack growth retardation near the crack tip in a metastable alloy [3,13], while in the hydrogen-containing environment, HE generally occurs and the hydrogen diffusion near a crack tip is more complex. Not only the hydrogen accumulates ahead of a loaded crack tip due to the stress assisted diffusion, but also a great amount of martensite transformation causes a sharp change in the hydrogen diffusion properties of the ASSs, i.e., the hydrogen diffusivity in martensite is about five orders of magnitude higher than that in austenite, while the solubility is about two orders of magnitude lower [14]. Chen et al. [3] investigated the hydrogen assisted fatigue crack growth (FCG) characteristics of ASSs with different austenite stability (301, 304L and 310S). The strain-induced martensite formed in the plastic zone ahead of the crack tip was responsible for the accelerated crack growth of the metastable stainless steels in hydrogen. Zhang et al. [6] characterized the hydrogen-induced crack initiation in hydrogen-charged metastable austenitic stainless steel, and it was experimentally found that the martensite not only provides a rapid hydrogen diffusion path but also promotes crack initiation. Wang et al. [15] conducted an FE analysis of hydrogen diffusion around the crack tip in austenitic stainless steel considering the SIMT. The presence of the martensite around a crack tip dramatically elevates the hydrogen concentration level.

It can be concluded that crack growth occurs at a lower stress level and fatigue crack growth rate is accelerated in the presence of the hydrogen [16–18]. The reasons are commonly attributed to the coupled effects of the SIMT and hydrogen near the crack tip. To date, the exact influence of the SIMT in conjunction with the stress–strain field on the local diffusion of hydrogen around the crack tip is not analyzed in detail in the current literature. One of the most important influence factors is the volume expansion caused by the austenite to martensite transformation. In our current understanding, the material volume increases as the austenite, with a face-centered cubic structure, changes into martensite, with a body-centered tetragonal structure. This volume expansion seriously affects the stress and strain distribution. For example, during the residual stress formation of the welded joint, the high tensile stress can be obviously decreased by this volume expansion, even changed into compressive stress field [19–21]. Similarly, the SIMT, while considering the volume change in metastable ASSs, inevitably causes the redistribution of stress and strain, and thus causes the redistribution of hydrogen concentration, especially near the crack tip. Unfortunately, such influences have never been reported in the current literature. Thus, the aim of this study is to reveal the influence of volume expansion of SIMT on the hydrogen diffusion around a crack tip. Hydrogen diffusion inside metal cannot be precisely predicted by methods, such as conventional experiment methods [22,23] and data-driven modeling [24–26]. Computational simulation technology may be the most powerful and efficient way [14,27,28]. In this study, a type 304L pressure vessel containing high-pressure hydrogen gas was used and FE analysis was conducted to intuitively investigate the hydrogen diffusion around a crack tip in this vessel.

2. Investigation Procedure

A pressure vessel, representing typical transport or storage containers for high-pressure hydrogen gas, with an inner surface crack tip was studied, as shown in Figure 1. The material used is a type 304L ASS which had been solution-annealed at 1080 °C for 1 h and water quenched with a yield stress of 201 MPa and tensile strength of 705 MPa. A mechanical hydrogen diffusion sequential coupled

procedure was built by using ABAQUS/Explicit 6.13 software with subroutines. The mechanical analysis was first conducted to obtain the stress–strain field considering the effect of SIMT along with its volume expansion. The yield stress was set to be associated with the flow rule and isotropic strain hardening following an experimentally true stress–strain curve [15]. The pressure stress and plastic strain were obtained around the crack tip. A user-defined field was used to present the strain-induced martensite fraction. The martensite fraction was calculated synchronously by the obtained plastic strain during the mechanical analysis. Furthermore, the volume expansion caused by the SIMT was implemented by a transformation expansion coefficient, set as 7.38×10^{-3} [20,29], multiplied the strain-induced martensite fraction. Next, the pressure stress field and martensite distribution results saved in the previous step were input as predefined fields into a mass diffusion simulation to obtain the hydrogen transient distribution. In this simulation, the hydrogen diffusion properties, i.e., hydrogen diffusivity and solubility were defined as a function of plastic strain and martensite fraction.

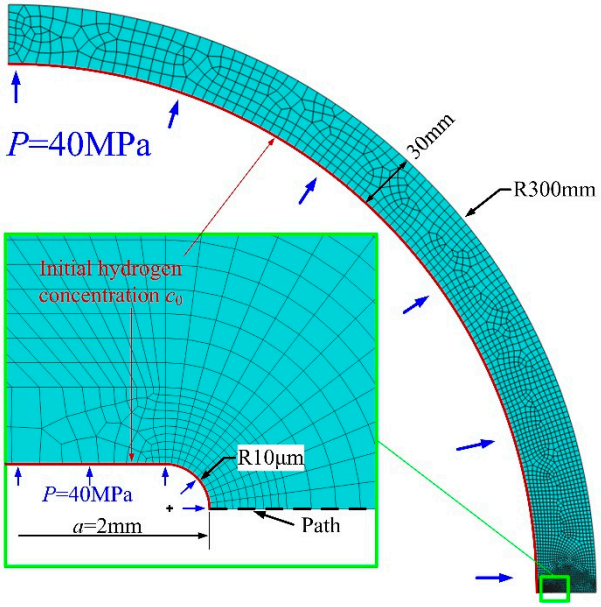

Figure 1. Mesh model and boundary conditions for the crack tip.

2.1. Hydrogen Dependent Material Properties

Based on the experiment results [15], the quantitative relation between the martensite f and plastic strain ε_p was shown as

$$\ln\left(\frac{f}{1-f}\right) = 2.538 \ln \varepsilon_p + 3.583. \tag{1}$$

Subsequently, a hydrogen diffusion evolution analysis was solved with the predefined fields of pressure stress field and martensite fraction field which were read from the previous analysis. As increasing the amount of martensite, the hydrogen diffusivity D increased while solubility s decreased. The equations were determined as [15].

$$\log D = \begin{cases} 0.352 \ln\left(\frac{f}{1-f}\right) - 13.877 & \text{for } \varepsilon_p \geq 0.1,\ f \geq 0.08 \\ -15.131 & \text{for } \varepsilon_p < 0.1,\ f < 0.08 \end{cases} \tag{2}$$

$$s = \begin{cases} 40.71f + 5.0 & \text{for } \varepsilon_p < 0.1,\ f < 0.08 \\ -6.19f + 8.71 & \text{for } \varepsilon_p \geq 0.1,\ f \geq 0.08 \end{cases}. \tag{3}$$

The hydrogen concentration of the inner surface c_0 was defined according to Sievert's law. Here, the initial concentration on the inner surface was evaluated to 36.0 ppm, and near the crack tip, decreased with the increase of martensite fraction.

2.2. Hydrogen Diffusion Analysis

The driving forces of hydrogen diffusion are a normalized concentration ϕ which is equal to the ratio of hydrogen concentration to solubility c/s, temperature gradient and pressure stress gradient, as shown in the governing equation [14,30–33]:

$$J = -sD\left\{\nabla\phi + \kappa_s\nabla[\ln(T - T_0)] + \kappa_p\nabla p\right\}, \tag{4}$$

where J is the flux of concentration of hydrogen, D and s are the hydrogen diffusivity and solubility, respectively. T is the temperature in Celsius and T_0 is the absolute zero. The Soret effect factor, κ_s, providing diffusion due to temperature gradient, is given by

$$\kappa_s = \frac{c(T - T_0)}{s^2}\frac{\partial s}{\partial T}. \tag{5}$$

Here, the simulations do not relate to the thermal-mechanical coupling, thus the Soret effect equals zero. The pressure stress factor, κ_p, providing diffusion driven by the gradient of the equivalent stress p, is shown as

$$\kappa_p = \frac{\overline{V_H}\phi}{R(T - T_0)}\ \text{mm N}^{-1/2} \tag{6}$$

where R is the universal gas constant, $\overline{V_H} = 2.0 \times 10^3$ mm^3/mol is the partial molar volume of the hydrogen in iron-based metals [34].

3. Results and Discussions

The mechanical analysis results considering the volume expansion of the SIMT, and then without considering the volume expansion, are shown in Figure 2. The martensite fraction distributions around the crack tip were similar in both calculations, indicating that the volume expansion has less effect on the SIMT, as well as plastic strain. However, the stress distributions were greatly changed, both in uniaxial stress and pressure stress. The maximum of the opening stress was decreased and more importantly, the stress of the crack tip adjacent to the inner hydrogen environment was changed from tensile stress into pressure stress. The stress field was completely changed in not only value, but also distribution contoured near the crack tip.

Figure 3 gives the stress and strain distributions along a path length (as shown in Figure 1). Apparently, the stress level and value were dramatically impacted by the volume expansion, as shown in Figure 3a. The stress concentration factor was partially relieved, especially at the crack tip with a pressure stress change of about 700 MPa. The volume expansion had very limited influence on the plastic strain field around the crack tip, as well as the martensite transformation fraction, as shown in Figure 3b,c, respectively. The differences were less than 5%. That attributes to the volume expansion amount used here, 7.38×10^{-3}, was far smaller than the maximum of plastic strain, ~0.4. Moreover, the effective length of the SIMT along the crack propagation direction was less than 0.03 mm. In this length range, with the influence of SIMT, the plastic strain and martensite transformation fraction were decreased at the tip and gradually changed to increase with the distance away from the tip.

Around the crack tip, the plastic strain caused by the external load directly induces the martensite transformation, then the martensite fraction directly changes the stress distribution according to its volume expansion. Conversely, stress change has a limited effect on the plastic strain and martensite fraction. However, for hydrogen diffusion, the most concerning factor is the stress gradient, as also

seen in Equation (4). The SIMT dramatically increased the stress gradient along the crack propagation direction and acted as another path for accelerating the hydrogen diffusion.

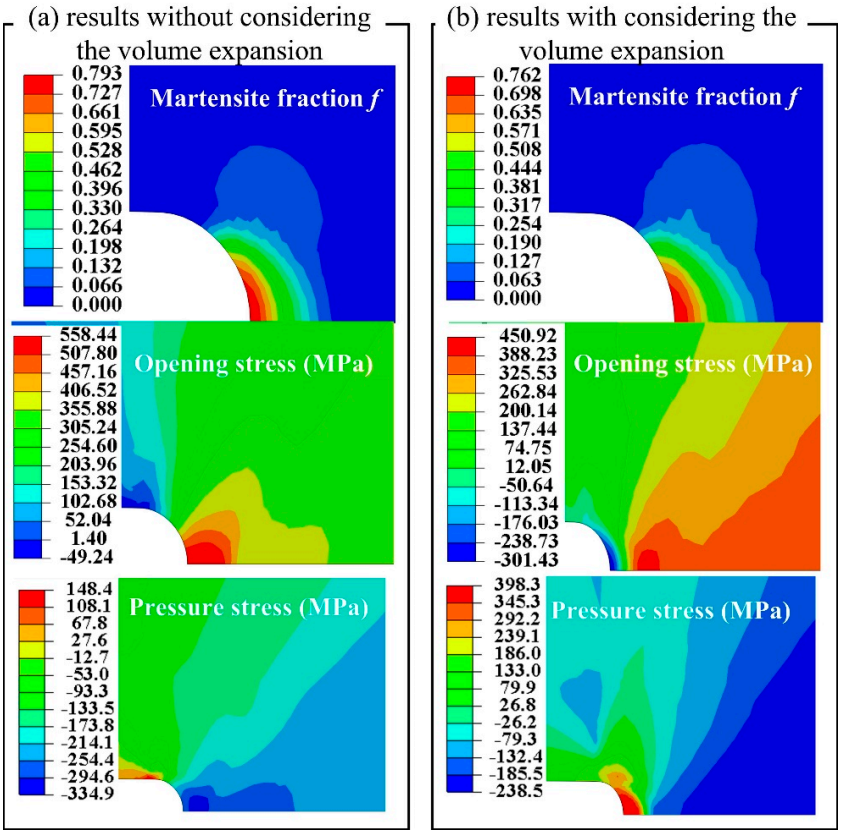

Figure 2. Mechanical analysis results around the crack tip. (**a**) Simulation results without considering the volume expansion and (**b**) simulation results considering the volume expansion.

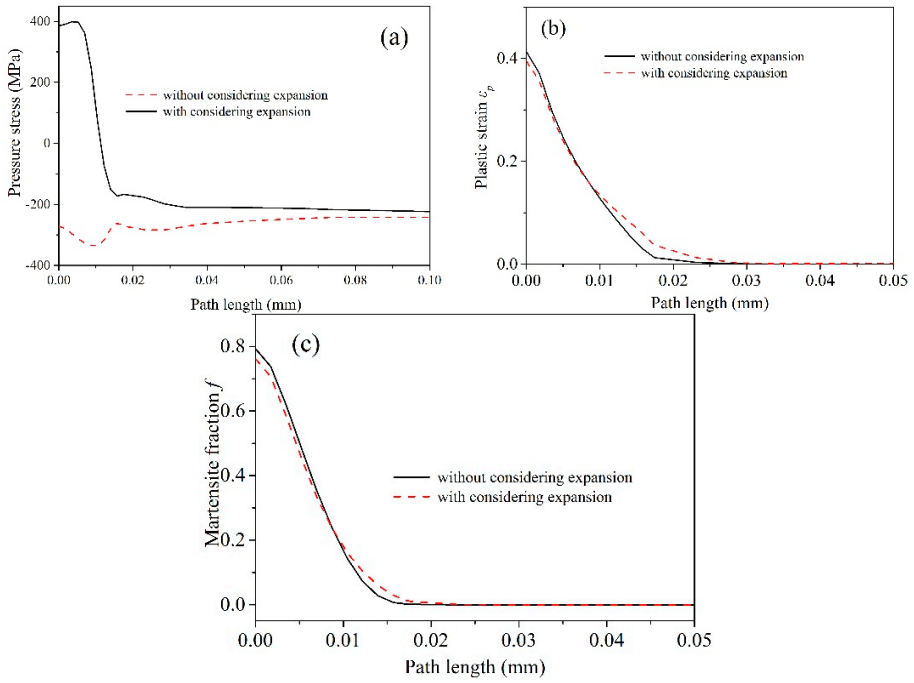

Figure 3. Stress (**a**), strain (**b**) and martensite fraction (**c**) comparisons along the path length away from the crack tip.

Figure 4 shows the hydrogen concentration evolutions around the crack tip. When the hydrogen concentration approached a steady-state, as shown in Figure 4a and b, the maximum hydrogen concentrations in both cases (with and without considering the effect of volume expansion) were located at the austenite side next to the induced martensite zone, rather than the martensite zone near the crack tip, which consistent with the experiment results [6,35]. The reason was that the strain-induced martensite rapidly transported the hydrogen atoms from the inner surface to the adjacent austenite for the higher diffusivity of the martensite [17]. However, the difference of the maximum concentration value in the two cases was obvious, i.e., 86.8 ppm versus 63.6 ppm, indicating that the volume expansion of the SIMT can largely increase the hydrogen concentration level. A comparable hydrogen diffusion analysis was conducted only considering the stress-assisted diffusion, which is also shown in Figure 4c. Apparently, the influence of the SIMT along with its volume expansion was much larger than the stress, showing that hydrogen accumulation was orders of magnitude faster.

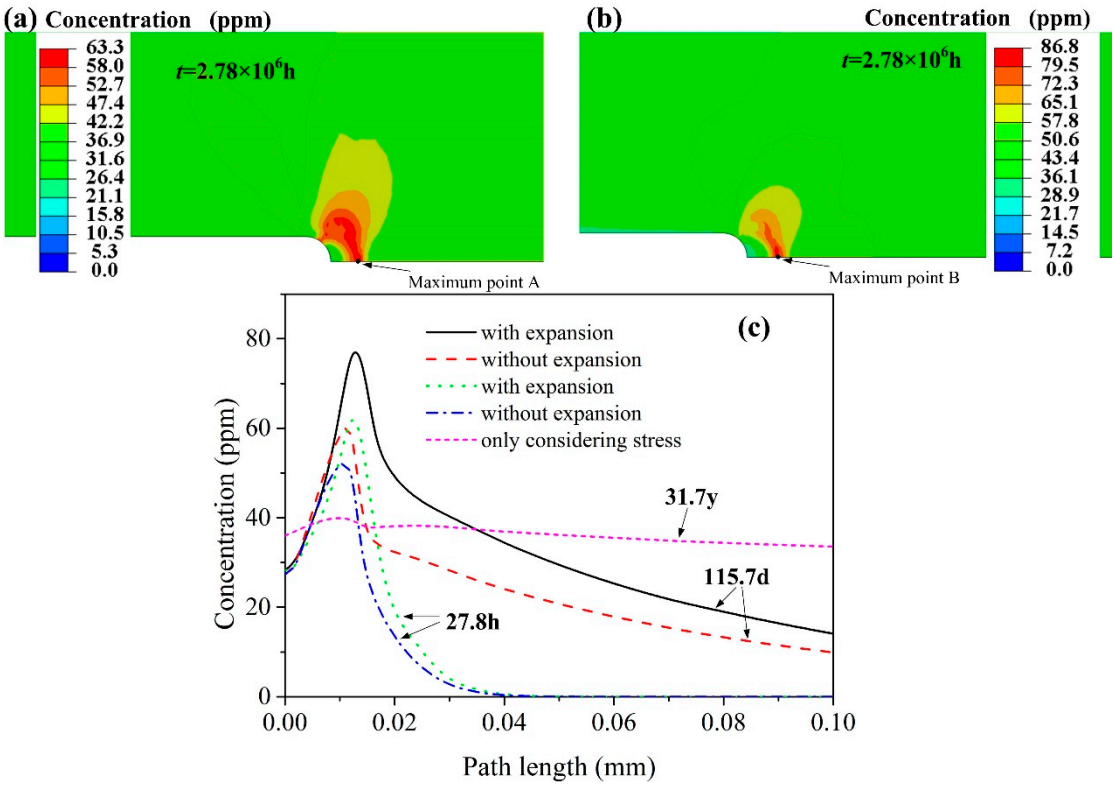

Figure 4. Hydrogen concentration results. (**a**) Hydrogen distribution without considering the volume expansion, (**b**) hydrogen distribution with considering the volume expansion and (**c**) comparison of the concentration along the path.

Due to the large differences of the hydrogen diffusivity and solubility of the austenite and martensite phase, the hydrogen from the inner-face diffused transiently, but the hydrogen accumulation was deterministic. The critical position with the maximum hydrogen concentration located at the site in the austenite rich region with a martensite fraction approximates to 0.1. The martensite fraction at the critical positions in both cases were the same as point A and B in Figure 4a,b, respectively. It could be deduced that the critical position was always at a position where the phase proportion was relatively constant. If the external force changed the SIMT area, the accumulation position changed. The volume expansion had an effect that the position with $f = 0.1$ was pulled back from the crack tip, thus the maximum concentration position was deeper.

Figure 5 shows the time evolution of hydrogen concentration at critical positions. The strain-induced martensite could accelerate the hydrogen diffusion, and considering the volume expansion, the hydrogen concentration approached a larger value. The martensite fraction was slightly decreased

with the influence of SIMT, and the hydrogen diffusivity in martensite phase was several orders of magnitude larger than that in austenitic phase. The hydrogen diffusivity of the material at the crack tip, while considering the volume expansion, was decreased. Thus, before the critical time, as shown in Figure 5, the hydrogen concentration, while considering the volume expansion, was lower than that without considering the expansion. After the critical time, the hydrogen concentration, while considering the expansion, became larger due to the larger stress gradient caused by the expansion. It is worth noting that a slight change of the martensite fraction causes obvious hydrogen diffusion behavior around the crack tip.

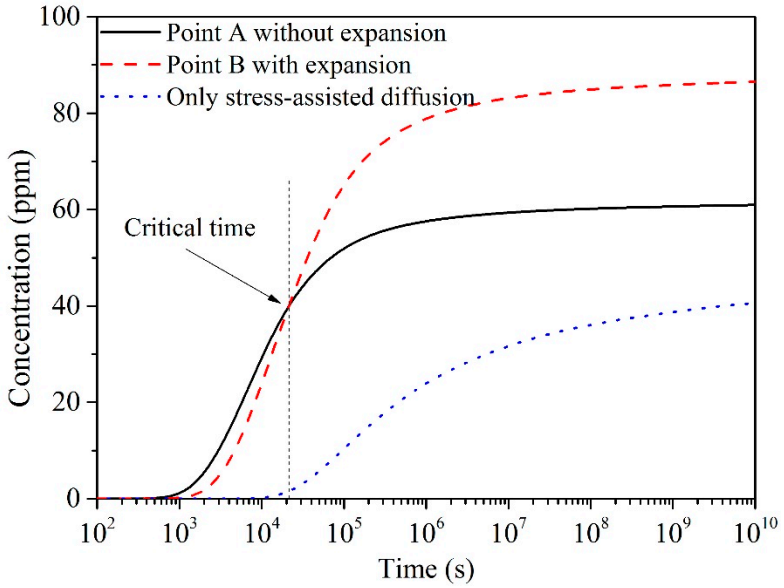

Figure 5. Evolution of hydrogen concentration at the critical position of the crack tip, where point A and B were the maximum concentration points in Figure 4.

The volume expansion of the SIMT had positive influences on the crack tip in the absence of hydrogen, such as it decreased stress concentration, changed the tensile stress into compression stress, retarded the plastic strain and martensite fraction (although limited). The volume expansion seemed to play an active role in the resistance to HE in mechanics. On the contrary, the hydrogen diffusion modeling found that the volume expansion of the SIMT increased the HE susceptibility. The volume expansion could not cause obvious change of the martensite fraction due to its small amount compared with the plastic strain, thus the hydrogen diffusivity was less affected. However, the stress field was very easy to be affected, only a nonzero volume expansion could change the stress distribution. To release the tensile stress or change to compressive stress, the stress–strain curve follows linear elastic constitutive relation, even the material was in the strain-hardening state. According to the stress results, as shown in Figure 2, the maximum tensile stress was no more than 500 MPa, thus, the needed strain to change the tensile state of the crack tip to compressed state was just 1–2 $\times$ 10^{-3}. Compared with the volume expansion strain (7.8 $\times$ 10^{-3}), the tensile stress around the crack tip is very easy to change to compressive stress under the effect of the volume expansion of SIMT. Once tensile stress around the crack tip was changed into severe compressive stress state, and the stress gradient was sharply increased, as shown in Figure 2. As results, the hydrogen diffusion was further accelerated.

Above all, the presence of SIMT elevated the level that the maximum hydrogen concentration reached—i.e., increased the HE susceptibility—in two ways. Firstly, a large amount of strain-induced martensite formed in the vicinity of the crack tip acted as a rapid path for hydrogen diffusion [3,17]. Secondly, the volume expansion of austenite to martensite phase transformation caused a great stress gradient from the crack tip point with pressure stress to the deeper maximum tensile stress position. This effect not only further accelerated the hydrogen transport to the critical position ahead of the crack

tip, but also further increased the maximum value of the hydrogen concentration at the critical position. The austenite at the critical position where hydrogen concentration had the maximum value was located at the austenite side near the SIMT zone was possibly embrittled by the high hydrogen concentration. Furthermore, this position had also contained an amount of martensite (f = 0.1), which could have been the micro-crack source. Thus, this critical position was probably destroyed with the combination of high hydrogen concentration, SIMT and stress field, consequently causing crack propagation.

The volume expansion of SIMT causes compressive stress in the martensite phase, while tensile stress in the austenite phase, therefore, large stress gradient was caused not only around the crack tip, but also in the phase interface between austenite and martensite. Once the ASSs were in the hydrogen environment, the hydrogen accumulation must happen in the phase interface and thus increases the susceptibility of HE. However, in the opening literature, suitable martensite transformation has a positive effect on ASSs. This conflicting effect of SIMT should be further investigated for the application of ASSs in a hydrogen environment.

4. Conclusions

The influence of the volume expansion of SIMT on the hydrogen diffusion around a crack tip of type 304L austenite stainless steel was investigated by building a mechanical hydrogen diffusion sequential coupled model. This volume expansion slightly influenced the plastic strain and martensite transformation fraction, so it has a very limited effect on the hydrogen diffusion properties around the crack tip. However, it severely affected the stress field distribution, i.e., changed the tensile stress state to high compressive stress state at the crack tip. A very large stress gradient was the result. Consequently, it further accelerated the transport and accumulation of the hydrogen from the inner surface towards a critical region ahead of the crack tip. The peak hydrogen concentration at the critical position located at the site in austenite-rich region where the martensite fraction approximated to 0.1. Compared to the analysis without considering the volume expansion, the effect of volume expansion further increased the susceptibility of HE.

Author Contributions: Methodology, Y.L. and Y.K.; writing—original draft preparation, Z.X.; writing—review and editing, W.Z.; visualization, J.Y.; supervision, Y.L., Y.K. and J.Y.

Funding: State Key Laboratory of Nuclear Power Safety Monitoring Technology and Equipment, grant number K-A2018.427 and National Natural Science Foundation of China, grant number 51705461.

Conflicts of Interest: The authors declare no conflict of interest.

References

1. Garcia, C.; Martin, F.; De Tiedra, P.; Alonso, S.; Aparicio, M.L. Stress corrosion cracking behavior of cold-worked and sensitized type 304 stainless steel using the slow strain rate test. *Corrosion* **2002**, *58*, 849–857. [CrossRef]
2. Lai, C.L.; Tsay, L.W.; Kai, W.; Chen, C. Notched tensile tests of cold-rolled 304L stainless steel in 40 wt.% 80 °C $MgCl_2$ solution. *Corros. Sci.* **2009**, *51*, 380–386. [CrossRef]
3. Chen, T.C.; Chen, S.T.; Tsay, L.W. The role of induced α'-martensite on the hydrogen-assisted fatigue crack growth of austenitic stainless steels. *Int. J. Hydrogen Energy* **2014**, *39*, 10293–10302. [CrossRef]
4. Ueki, S.; Mine, Y.; Takashima, K. Crystallographic study of hydrogen-induced twin boundary separation in type 304 stainless steel under cyclic loading. *Corros. Sci.* **2017**, *129*, 205–213. [CrossRef]
5. Jackson, H.; San Marchi, C.; Balch, D.; Somerday, B.; Michael, J. Effects of low temperature on hydrogen-assisted crack growth in forged 304L austenitic stainless steel. *Metall. Mater. Trans. A* **2016**, *47A*, 4334–4350. [CrossRef]
6. Zhang, L.; An, B.; Fukuyama, S.; Iijima, T.; Yokogawa, K. Characterization of hydrogen-induced crack initiation in metastable austenitic stainless steels during deformation. *J. Appl. Phys.* **2010**, *108*, 063526. [CrossRef]

7. Chen, X.; Zhou, C.; Cai, X.; Zheng, J.; Zhang, L. Effects of external hydrogen on hydrogen transportation and distribution around the fatigue crack tip in type 304 stainless steel. *J. Mater. Eng. Perform.* **2017**, *26*, 4990–4996. [CrossRef]
8. Sofronis, P.; McMeeking, R.M. Numerical analysis of hydrogen transport near a blunting crack tip. *J. Mech. Phys. Solids* **1989**, *37*, 317–350. [CrossRef]
9. Toshimitsu, Y.J.A.; Takenao, N.; Koji, S.; Tetsuya, Y. Numerical analysis on hydrogen diffusion and concentration in solid with emission around the crack tip. *Eng. Fract. Mech.* **1996**, *55*, 47–60.
10. Liang, Y.; Sofronis, P. Toward a phenomenological description of hydrogen-induced decohesion at particle/matrix interfaces. *J. Mech. Phys. Solids* **2003**, *51*, 1509–1531. [CrossRef]
11. Takakuwa, O.; Nishikawa, M.; Soyama, H. Numerical simulation of the effects of residual stress on the concentration of hydrogen around a crack tip. *Surf. Coat. Technol.* **2012**, *206*, 2892–2898. [CrossRef]
12. Martínez-Pañeda, E.; del Busto, S.; Niordson, C.F.; Betegón, C. Strain gradient plasticity modeling of hydrogen diffusion to the crack tip. *Int. J. Hydrogen Energy* **2016**, *41*, 10265–10274. [CrossRef]
13. Mayer, H.R.; Stanzl-Tschegg, S.E.; Sawaki, Y.; Huhner, M.; Hornbogen, E. Influence of transformation-induced crack closure on slow fatigue crack growth under variable amplitude loading. *Fatigue Fract. Engngy Mater. Struct.* **1995**, *19*, 935–948. [CrossRef]
14. Olden, V.; Saai, A.; Jemblie, L.; Johnsen, R. FE simulation of hydrogen diffusion in duplex stainless steel. *Int. J. Hydrogen Energy* **2014**, *39*, 1156–1163. [CrossRef]
15. Wang, Y.; Li, X.; Dou, D.; Shen, L.; Gong, J. FE analysis of hydrogen diffusion around a crack tip in an austenitic stainless steel. *Int. J. Hydrogen Energy* **2016**, *41*, 6053–6063. [CrossRef]
16. Kanezaki, T.; Narazaki, C.; Mine, Y.; Matsuoka, S.; Murakami, Y. Effects of hydrogen on fatigue crack growth behavior of austenitic stainless steels. *Int. J. Hydrogen Energy* **2008**, *33*, 2604–2619. [CrossRef]
17. Wang, Y.; Wang, X.; Gong, J.; Shen, L.; Dong, W. Hydrogen embrittlement of catholically hydrogen-precharged 304L austenitic stainless steel: Effect of plastic pre-strain. *Int. J. Hydrogen Energy* **2014**, *39*, 13909–13918. [CrossRef]
18. Hallberg, H.; Banks-Sills, L.; Ristinmaa, M. Crack tip transformation zones in austenitic stainless steel. *Eng. Fract. Mech.* **2012**, *79*, 266–280. [CrossRef]
19. Jiang, W.; Chen, W.; Woo, W.; Tu, S.-T.; Zhang, X.-C.; Em, V. Effects of low-temperature transformation and transformation-induced plasticity on weld residual stresses: Numerical study and neutron diffraction measurement. *Mater. Design* **2018**, *147*, 65–79. [CrossRef]
20. Wang, Q.; Liu, X.S.; Wang, P.; Xiong, X.; Fang, H.Y. Numerical simulation of residual stress in 10Ni5CrMoV steel weldments. *J. Mater. Process. Tech.* **2017**, *240*, 77–86. [CrossRef]
21. Zheng, W.J.; He, Y.M.; Yang, J.G.; Gao, Z.L. Hydrogen diffusion mechanism of the single-pass welded joint in welding considering the phase transformation effects. *J. Manuf. Process.* **2018**, *36*, 126–137. [CrossRef]
22. Kim, Y.S.; Kim, S.S.; Choe, B.H. The role of hydrogen in hydrogen embrittlement of metals: the case of stainless steel. *Metals* **2019**, *9*, 406. [CrossRef]
23. Martinez, B.A.; Laso, J.A.A.; Gutierrez-Solana, F.; Martinez, A.C.; Martinez, Y.J.J.; Aparicio, A.R.S. A proposal for the application of failure assessment diagrams to subcritical hydrogen induced cracking propagation processes. *Metals* **2019**, *9*, 670. [CrossRef]
24. Zheng, W.J.; Liu, Y.; Gao, Z.L.; Yang, J.G. Just-in-time semi-supervised soft sensor for quality prediction in industrial rubber mixers. *Chemom. Intell. Lab. Syst.* **2018**, *180*, 36–41. [CrossRef]
25. Liu, Y.; Yang, C.; Gao, Z.; Yao, Y. Ensemble deep kernel learning with application to quality prediction in industrial polymerization processes. *Chemom. Intell. Lab. Syst.* **2018**, *174*, 15–21. [CrossRef]
26. Xuan, Q.; Chen, Z.; Liu, Y.; Huang, H.; Bao, G.; Zhang, D. Multiview generative adversarial network and its application in pearl classification. *IEEE Trans. Ind. Electron.* **2019**, *66*, 8244–8252. [CrossRef]
27. Zheng, W.; He, Y.; Yang, J.; Gao, Z. Influence of crystallographic orientation of epitaxial solidification on the initial instability during the solidification of welding pool. *J. Manuf. Process.* **2019**, *38*, 298–307. [CrossRef]
28. Beldowski, P.; Mazurkiewicz, A.; Topolinski, T.; Malek, T. Hydrogen and water bonding between glycosaminoglycans and phospholipids in the synovial fluid: Molecular dynamics study. *Materials* **2019**, *12*, 2060. [CrossRef]
29. Deng, D. FEM prediction of welding residual stress and distortion in carbon steel considering phase transformation effects. *Mater. Design* **2009**, *30*, 359–366. [CrossRef]

30. Olden, V.; Alvaro, A.; Odd, M.A. Hydrogen diffusion and hydrogen influenced critical stress intensity in an API X70 pipeline steel welded joint—Experiments and FE simulations. *Int. J. Hydrogen Energy* **2012**, *27*, 11474–11486. [CrossRef]
31. Alvaro, A.; Olden, V.; Akselsen, O.M. 3D cohesive modelling of hydrogen embrittlement in the heat affected zone of an X70 pipeline steel. *Int. J. Hydrogen Energy* **2013**, *38*, 7539–7549. [CrossRef]
32. Yan, C.; Liu, C.; Yan, B. 3D modeling of the hydrogen distribution in X80 pipeline steel welded joints. *Comp. Mater. Sci.* **2014**, *83*, 158–163. [CrossRef]
33. Toribio, J.; Kharin, V.; Vergara, D.; Lorenzo, M. Two-dimensional numerical modelling of hydrogen diffusion in metals assisted by both stress and strain. *Adv. Mater. Res.* **2010**, *138*, 117–126. [CrossRef]
34. Serebrinsky, S.; Carter, E.A.; Ortiz, M. A quantum-mechanically informed continuum model of hydrogen embrittlement. *J. Mech. Phys. Solids* **2004**, *52*, 2403–2430. [CrossRef]
35. Mine, Y.; Koga, K.; Kraft, O.; Takashima, K. Mechanical characterisation of hydrogen-induced quasi-cleavage in a metastable austenitic steel using micro-tensile testing. *Scr. Mater.* **2016**, *113*, 176–179. [CrossRef]